Materials Research. 2022; 25:e20220304
DOI: https://doi.org/10.1590/1980-5373-MR-2022-0304

Optoelectronic Properties of Bismuth Sulfide Thin Films Grown by PVD

J. Cruz-Gómez[a], E.B. Cruz-Díaz[a], D. Santos-Cruz[b], Aruna-Devi Rasu Chettiar[a], S. A. Mayén-Hernández[a], F. de Moure-Flores[a], M. Vega-González[c], C.E. Pérez-García[a], A. Centeno[d], José Santos-Cruz[a]*

[a]Universidad Autónoma de Querétaro, Facultad de Química, Posgrado en Energía, México.
[b]Departamento de Ingeniería Eléctrica, Sección de Electrónica del Estado Sólido, Cinvestav-IPN, Ciudad de México, México.
[c]Universidad Nacional Autónoma de México, Centro de Geociencias, Boulevard Juriquilla, Querétaro, México.
[d]Universidad de Guadalajara, Departamento de Física, Centro Universitario de Ciencias Exactas e Ingenierías, Guadalajara, México.

Received: July 04, 2022; Revised: August 22, 2022; Accepted: September 26, 2022

Bismuth (III) sulfide thin films are prepared on glass substrates by physical vapor deposition technique. Then, the films are annealed at different temperatures from 150 to 350°C with nitrogen and nitrogen-sulfur atmospheres, respectively. The effect of annealing temperature on the optoelectronic properties is investigated. The layers were characterized using ultraviolet-visible spectroscopy, XRD, Raman spectroscopy, EDS analysis and Hall effect. The film annealed at 250°C in a nitrogen-sulfur atmosphere exhibited the best condition with an initial thickness of 106 nm and band gap of 1.37 eV. Also, Bismuthinite phase was obtained, close to the stoichiometry with 59.95 and 40.05 at % for bismuth and sulfur, respectively. The charge carrier concentration of $6.9x10^{19}$ cm^{-3} with a n-type conductivity, the resistivity of 0.19 Ω-cm, and mobility of 0.44 $cm^2V^{-1}s^{-1}$ are obtained.

Keywords: *Bismuth sulfide, Physical vapor deposition, Thermal Annealed, Optoelectronic Properties.*

1. Introduction

Nowadays its most frequently find heavy metal in great variety of materials such as thin films and powders, for instance cadmium and lead, in various even medical applications[1]. The risk of using toxic semiconductor materials is becoming increasingly apparent; both in water[2] and in air[3,4] and even in our food[2]. Several non-toxic semiconductor materials are being studied, such as zinc oxide (ZnO)[5].One champion material within the field of use of semiconductor is a non-toxic material, cheap and environmental friendly; bismuth sulfide, which has optical and electrical properties suitable for use in sensors, photocatalysis, photodiodes, solar cells and as a thermoelectric material[1,6]. These properties are: n-type semiconductor, bandgap 1.3 eV, high absorption coefficient of $10^4 – 10^5$ cm^{-1}, intrinsic carriers concentration of 3×10^{18} cm^{-3}, electron mobility of 200 cm^2 V^{-1} s^{-1}, electrical conductivity of $10^{-6} – 10^{-7}$ Ω^{-1} cm^{-1}, and hole mobility[7] of 1100 cm^2 V^{-1} s^{-1}. The orthorhombic crystal structure of bismuth sulfide (Bismuthinite) includes two bismuth centers of different coordination number, these units form continuous chains along the c-axis, when joined by Van der Walls links with those of the other unit cells[8].

When bismuth sulfide is deposited in thin films, the value of its bandwidth forbidden varies from 1.2 to 1.7 eV[9] and since its energy from the edge of its conduction band is located, approximately, in 4.35 eV and that of valence in 5.65 eV[10]. It is possible to use thin films of bismuth sulfide for photovoltaic applications. This is carried out in various ways, one of them is in dye sensitized solar cells, also in bilayer cells of quantum dots, another in hybrid solar cells bilayer, and finally, in the form of electron transport layer in organic and hybrid cells[11].

The synthesis and deposit of this material are diverse. Within chemical techniques is widely used chemical synthesis using one or more precursors; same that generate the ionic species Bi^{3+} and S^{2-} which join to form the crystals of the material. The solvothermal process is also used, working with organic solvents, like the hydrothermal process. Another medium is the synthesis by sol-gel, which in its initial process forms a colloidal suspension, usable to deposit thin films by various techniques, which then forms a gel. Even films can be grown by electrochemical deposit. Within physical processes, it is possible to grow thin films by sputtering; pyrolysis spray, electron gun evaporation and vacuum evaporation, among others[7,12-15] Vacuum evaporation is a simple, replicable and fast technique used to deposit thin films from high purity materials[16]. In this work the vacuum evaporation technique was used to deposit satisfactory thin layers of bismuth sulfide, polycrystalline, very close to the stoichiometry of the compound, and with good electro-optical properties; this technique has been little used, although it has the advantage of being highly reproducible[17]. According to

*e-mail: jsantos@uaq.edu.mx

the theory of this deposition technique, better properties are to be expected in the films deposited at higher amperages, since the evaporated molecules have a higher energy, and a better accommodation on the substrate surface[18]. The films obtained were thermal annealed in two atmospheres nitrogen and nitrogen-sulfur respectively at 250 to 350 °C in steps of 50 °C. The films obtained were characterized by UV-Vis spectroscopy, Raman spectroscopy, X-ray diffraction, SEM and profilometry.

2. Materials and Methods

All the samples were evaporated in a PVD equipment, the source of Bi_2S_3 powder, and was obtained by the microwave synthesis as follow. All reagents were used as received without further purification. Bismuth chloride ($BiCl_3$, Sigma Aldrich) were used as the sources of bismuth, and thioacetamide (TA) (Fermont) as the source of sulfur. Ethylene glycol (EG) was used as solvent. The solvent volume in all cases was of 50 mL, unless otherwise is mentioned. The concentration of $BiCl_3$ was 0.01 M, and the corresponding TA solution, 0.05 M. The reaction solutions were set under ultrasound shaking at room temperature for 10 min or until the salts were dissolved completely. Subsequently, the solutions were sealed in Teflon tubes (reactor) of 100 mL and placed inside the microwave oven (CEM MARS-6) under high-speed stirring. The temperature of the oven was set at a point 120°C, and the power of the oven at 600 W. The reaction and ramp time remained constant: 20 and 10 min., respectively. After the reaction, black Bi_2S_3 products were centrifuged, washed several times with ethanol and dried at room temperature.

The Bi_2S_3 material obtained was used as a powder source-tungsten boat in a physical vapor deposition equipment. The methodology followed was as follows, using the technique physical vapor deposition the thin films were grown with various thicknesses of bismuth sulfide on Corning glass substrates, previously treated with chromic mixture for 24 hours, and 3 hours with solution at boiling point 1: 3 (V:V) of nitric acid in water. For these growths, the distance between the substrate and the boat containing the material was 16 cm and was keep constant, the deposit time and the current applied to the molybdenum boat were varied from 60 to 130 amperes and 1-3 minutes. The films obtained were thermal annealed with nitrogen and sulfur atmosphere respectively at 150-350 °C in steps of 50 °C and a ramp of temperature of 15 °C/min.

3. Characterization

The characterization of the films obtained was achieved by UV-Vis using a UV-Vis spectrophotometer brand Thermo Scientific model Genesys 10S; X-ray diffractograms were obtained using a Rigaku model Ultima IV equipment with copper target using Kα radiation with a wavelength of 0.15418 nm, with a power of 40 KV; Raman spectra were obtained with Micro Raman equipment brand Thermo Scientific model DRX2 using red laser (λ = 633 nm); the surface morphology and stoichiometry of the films was studied by means of scanning electron microscope (SEM) with 20 kV electron high tension and energy dispersive X-ray (EDX) using Tescan Mira 3 FEG-SEM instrument and the layers thicknesses were measured using a KLA Tencor profiler model D-100.

4. Results and Discussion

Figure 1 display the diffraction patterns of the bismuth sulfide films, Figure 1a with thermal annealed treatment in a nitrogen atmosphere at room temperature 150, 200, 250, 300 and

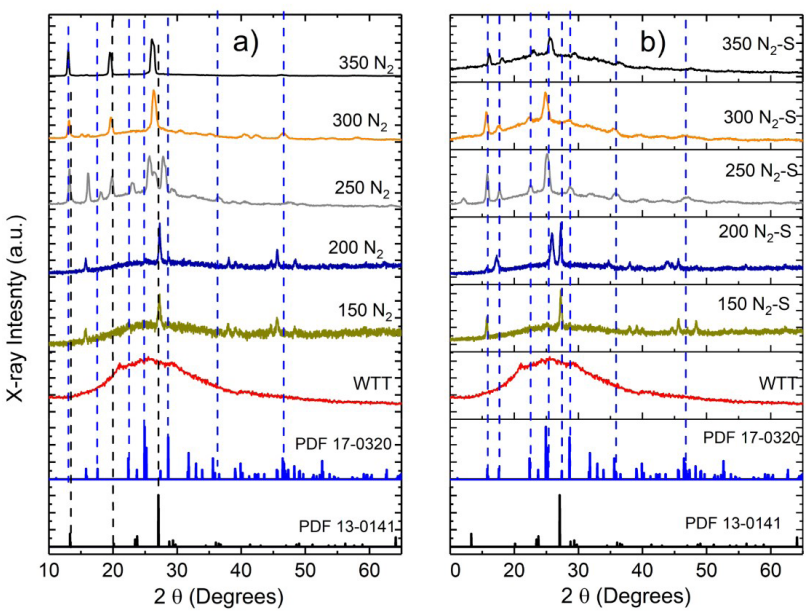

Figure 1. Diffractions patterns of the thin films of Bi_2S_3 with a thermal annealed at different temperatures: a) in a nitrogen atmosphere, and (b) nitrogen-sulfur atmosphere.

350 °C respectively and Figure 1b with thermal annealed in a nitrogen-sulfur atmosphere, at the same temperatures. The diffraction signals match well with the position with those of the reference PDF #17-0320 that correspond to Bismuthinite with chemical formula Bi_2S_3, orthorhombic phase and space group Pbnm (62) and PDF #13-0141 for Monoclinic sulfur and space group P21/c (14). Figure 1a films at room temperature display an amorphous material and the samples annealed at 150 and 200 °C, showed only a sulfur diffraction pattern with match very well with a PDF# 13-0141. At annealed temperatures of 250, 300 and 350 °C, the films shown a mixture of sulfur and bismuthinite phases respectively, this could be due the bismuth was evaporated with the temperature and only nitrogen atmosphere is not enough to keep the bismuth in the films. When the films annealed in a nitrogen-sulfur atmosphere at room temperature the films are amorphous, at 150 and 200°C the films have a mixture of sulfur and bismuthinite phases respectively, at 200 to 350°C the thin films match very well with the bismuthinite phase, at 350°C the film is thinning due to the thermal annealed temperature.

Figure 2 shows the thickness obtained at different thermal treatment temperatures and atmospheres. For the treatment in the nitrogen atmosphere, an almost linear correlation between thickness and temperature is obtained; only a slight deviation at 250°C. This behavior can be explained by the growth of the crystals that make up the film of the material; this growth occurs as the treatment temperature rises. In the case of the sulfur-nitrogen atmosphere, the behavior is not linear; it is quadratic, with a maximum of 250°C, and a slight deviation from this behavior when the treatment temperature is 200°C. This behavior can be the result of material loss when the treatment temperature exceeds 250°C. Observed as a whole, both curves show similar behavior; except when the treatment temperature rises above 300°C. It is above this temperature that the sulfur-nitrogen atmosphere favors the loss of material, while that of nitrogen does not.

Figure 3 shown a typical Raman spectrum from 100 to 400 cm^{-1} for bismuth sulfide thin films under 633 nm excitation laser, with thermal annealed treatments at six temperatures, 25°C (RT), 150 to 350 °C in a step of 50°C respectively Figure 3a) in a nitrogen and 3b) nitrogen-sulfur atmospheres, respectively. The samples with thermal annealed in nitrogen atmosphere shown only two vibrational modes that correspond to Bi_2S_3, B_{3u}, A_g and B_g that correspond not a complete formation of the bismuth sulfide, these results are consistent with the XRD for a nitrogen thermal annealed Figure 1a. Raman technique could identify microphases of compounds that XRD cannot, in the Raman results with nitrogen atmosphere the vibrational modes at 105.4, 122.54 and 138.89 cm^{-1} respectively are associated to alpha bismuth trioxide with chemical formula Bi_2O_3[19], by XRD analysis was not possible to identify the presence of this bismuth oxide.

In all the Raman Spectra (Figure 3b), two Ag vibrational modes located at 188 and 238 cm^{-1} Raman displacement. Also, B_g vibrational mode was observed at 262 cm^{-1} Raman displacement. This mode located at 262 cm^{-1} is due to the vibrations of the Bi-S bonds; while the modes at 188 and 238 cm^{-1} are due to the vibration of the surface phonon

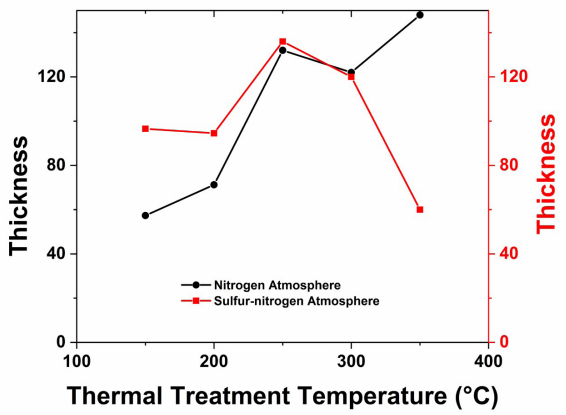

Figure 2. Thickness of thin films of Bi_2S_3 grown by PVD with different thermal treatments.

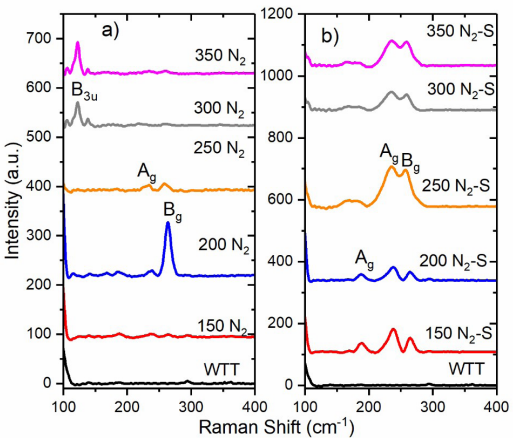

Figure 3. Raman spectra of Bi_2S_3 films grown by PVD a) annealed in a nitrogen atmosphere and b) annealed in a nitrogen-sulfur atmosphere, respectively.

and match well with the vibrational modes associated at Bi_2S_3[11]. The presence of a better bismuthinite phase is for 250, 300 and 350 °C temperatures and nitrogen-sulfur atmosphere, respectively.

Figure 4 shown the EDS results of the films annealed in a) nitrogen and b) nitrogen-sulfur atmospheres respectively, the figure displays results at annealed temperature of a 25, 150, 200, 250, 300 and 350°C, respectively. In Figure 4a all the samples annealed in a nitrogen atmosphere are away of the stoichiometry, for bismuth (black dashed and point line) and for sulfur (blue dashed and point line). The bismuth atomic percent diminishes as a temperature increase for 60 to 52 at %, and for sulfur increase as a temperature increase for 39 to 48 at % respectively. In a nitrogen atmosphere is evident that the stoichiometry is not reached and there is a deficiency of sulfur in all the films. Film annealed (Figure 4b) at nitrogen-sulfur atmosphere revealed the stoichiometry at 250°C, after this temperature the sulfur concentration increase as a function of temperature up to 67 atomic%, and the bismuth concentration diminishes as a function of annealed temperature up to 33 atomic%.

Figure 5 shows the UV-Vis spectra of the film annealed at different temperatures 25, 150-350°C in steps of 50°C and atmospheres, Figure 5a) nitrogen, Figure 5b) nitrogen-sulfur atmospheres respectively and Figure 5c) shows the compute of the forbidden bandwidth using Tauc method, it is known that electronic transitions are direct for the case of bismuth sulfide[8]. Bandwidth forbidden values are slightly higher than those considered by Ahire et al.[9]. Just above the maximum, which also the Tauc method is a useful estimate but usually presents these deviations. Figure 5a) show the transmittance spectra of 300 to 1000 nm, the transmittance values are 30% maximum for 300°C and the minimum value for room temperature and 150°C, Figure 5b) display at maximum transmittance value of 50% for 250°C and a minimum for room temperature, in both spectra series it could be observed an abrupt absorption edge for 250 to 350°C for nitrogen atmosphere and for nitrogen-sulfur atmosphere. For the band gap for nitrogen atmosphere the maximum value was for 150°C with 2.2 eV after this temperature the values diminishes with minimum value of 1.63 eV for annealed temperature of 300°C. For the annealed atmosphere of nitrogen-sulfur the values diminish for a 150°C with a minimum value of band gap of 1.82 eV, after this temperature the band gap increase up to 2.27 eV, for 350°C.

For UV-Vis, the band gap not match with the reported in the literature, in Figure 6 display the photoluminescence spectra of films annealed at 25, 250, 300 and 350°C in both atmospheres nitrogen Figure 6a) and nitrogen-sulfur Figure 6b), for an nitrogen atmosphere it appreciate that for 25°C (WTT), 250°C shown two peaks at 1.58 and 1.94 eV, in PL technique the maximum peak its associated to the band gap. For a nitrogen-sulfur atmosphere the maximum peak is observed at 1.37 eV, another peaks were also obtained at 1.58 and 1.93 eV.

Figure 7 displays the surface morphology of the thin films annealed an atmosphere of nitrogen-sulfur for 25, 250, 300 and 350°C respectively, at 25°C (Figure 7a) the aggregates are small, and is not present the formation of grains, Figure 7b annealed at 250°C the aggregates are of the order of 50-250 nm , for 350°C Figure 7c it could observed a most uniform aggregates and grain size of the order of 50 nm, at 350°C. Figure 7d consist of grains formed from coalescence and formation of nanostructures on the surface.

Figure 8 shown the hall results of thin films of bismuth sulfide annealed in a nitrogen atmosphere. Figure 8a shows a clear tendency of carrier concentration to increase as temperature does. Figure 8b shows the behavior of carriers' mobility, which, in general, decreases when the temperature decreases. In this case there is a discordance with the sample at 200°C, we can explain it by the behavior observed in the X-ray diffractogram, and by the Raman spectrum of said sample. We observed that this sample presents signals of the presence of the two crystalline phases, bismuthinite and monoclinic sulfur, this formation of both crystalline phases may be the cause of this low mobility not expected for this sample. This sample is the only one in the Raman series that presents the B_g mode of such intensity, and in X-rays it shows clear reflections of both crystalline phases. On the other hand, Figure 8c shows the behavior of the resistivity, which is very stable, considering the samples at the various

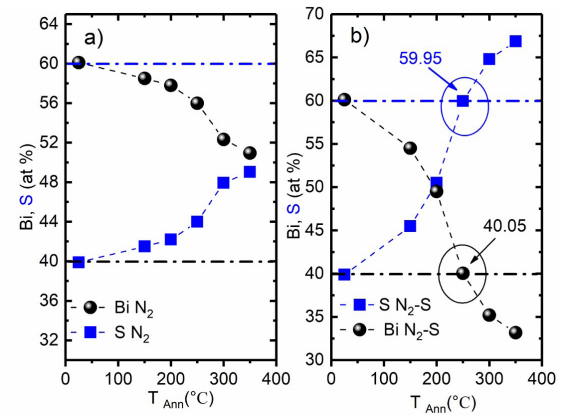

Figure 4. EDS results of Bi_2S_3 thin films annealed in an a) nitrogen and b) nitrogen-sulfur atmospheres, as a function of temperature.

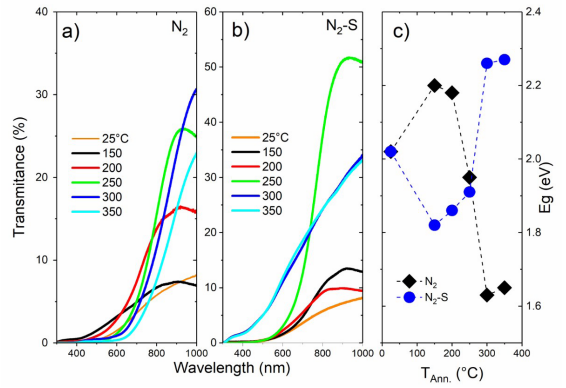

Figure 5. UV-Vis spectra of the film annealed at room temperature and five temperatures: a) In a nitrogen atmosphere, b) in a nitrogen-sulfur atmosphere and c) Direct Band gap as a function of the temperature and atmospheres.

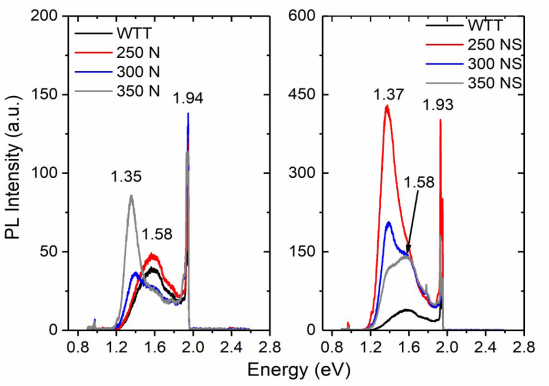

Figure 6. Photoluminescence spectra of the film annealed at different a) In a nitrogen atmosphere, b) in a nitrogen-sulfur atmosphere, respectively.

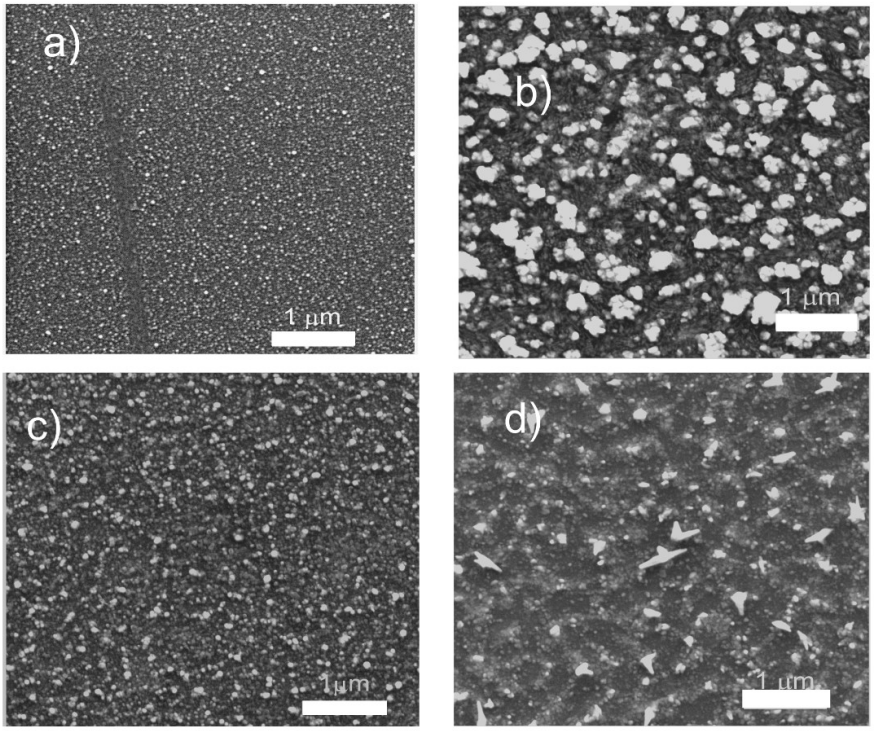

Figure 7. SEM images of the Bi_2S_3 thin films annealed in a nitrogen-sulfur atmosphere at a) 25°C, b) 250°C, c) 300°C and c) 350°C, respectively.

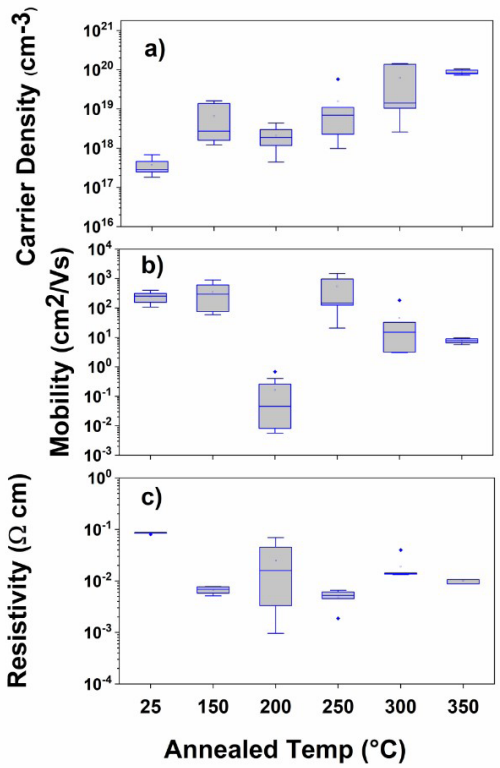

Figure 8. Hall effect results for the nitrogen annealed layers of Bi_2S_3 at different temperatures a) carrier density, b) mobility and c) resistivity.

treatment temperatures; practically remains unchanged, the differences are within the variation of the observed data, with an approximate value of 8×10^{-3} Ωcm.

Figure 9 shown the hall results of thin films of bismuth sulfide annealed in a nitrogen-sulfur atmosphere. Figure 9a shows the behavior of the carrier concentration; in general, it has a maximum for the sample with heat treatment at 250°C. In correspondence in Figure 9b shows a behavior, in general terms, opposite of the mobility of carriers. It has a minimum at 250°C. This maximum and this minimum can be associated with the EDS results, in which the best approximation to the stoichiometric atomic relationship of Bi_2S_3 is observed at 250°C. Like nitrogen treatment an unexpected variation at 200°C we also observed in the nitrogen-sulfur treatment; where the concentration of carriers is lower than expected and consequently the mobility increases. When observing the Raman spectrum, signals of lower intensity are noticeable with respect to the anterior and posterior samples; while the X-ray diffractogram shows, again, the presence of the two mentioned phases, so that the presence of the two phases and the low crystallinity with respect to the nearby samples generate this variation for the sample at 200°C. On the other hand, Figure 9c shows the behavior of resistivity; which behaves without significant variation up to the temperature of 250°C; which is the temperature where the atomic relationship closest to the stoichiometric is achieved, the resistivity value in this first zone is in the order of 10^{-1} Ωcm. After 250°C the resistivity increases to a value of 10 Ωcm.

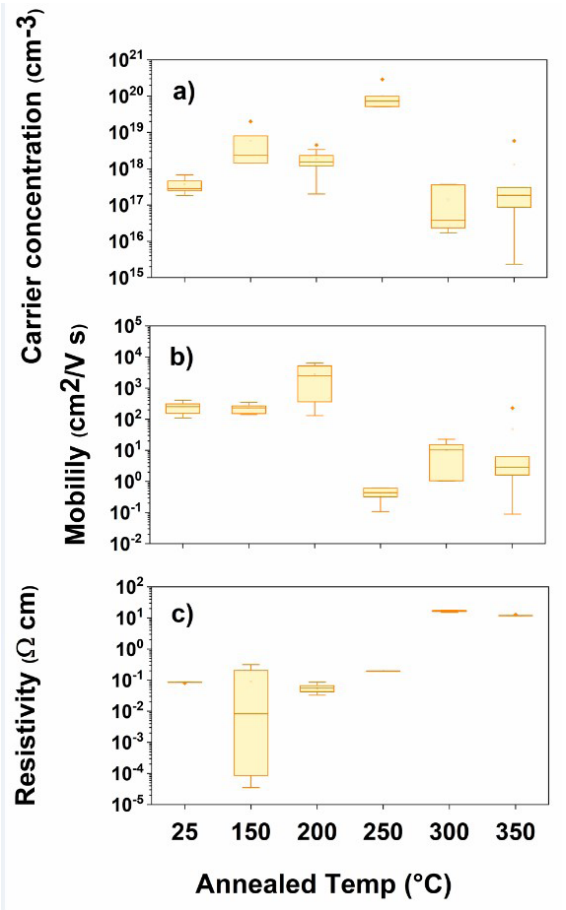

Figure 9. Hall effect results for the nitrogen-sulfur annealed layers of Bi_2S_3 at different temperatures a) carrier density, b) mobility and c) resistivity.

5. Conclusion

The options for using these films in solar cells are several. One of them is as an n-type semiconductor in quantum dot solar cells, the drawback is that typical semiconductor materials involve the use of lead or cadmium. In cadmium telluride solar cells; it can displace cadmium sulfide as an n-layer, but cadmium would remain in tellurium. Another option is to use them in bilayer organic solar cells; but given the nature of p-type semiconductor polymers, low diffusion length of photogenerated excitons, the p-type layer would be very thin (less than 30 nm) and the efficiency in power conversion would be negligible. A viable and less toxic option would be to use these films as an electron transport layer in organic and hybrid cells, and even in lead-free perovskite cells. This last option is viable given the good mobility of electrons, much higher than that of normally used materials, such as zinc oxide, titanium dioxide, PFN polymer and others. In addition, it has a conduction band at the height of that of fluorine doped tin oxide (FTO) and approximately 0.5 eV above indium and tin oxide, so during electron transport there will be little or no recombination.

Therefore, the films obtained through the PVD technique are recommended to be used in organic and hybrid solar cells; with polymers such as PTB7 and P3HT or similar. We suggest that these films be used as an electron transport layer (ETL), with optimal thickness to be determined, with an initial value between 30 and 50 nm.

6. References

1. Najahi-Missaoui W, Arnold RD, Cummings BS. Safe nanoparticles: are we there yet? Int J Mol Sci. 2021;22(1):1-22. http://dx.doi.org/10.3390/ijms22010385.
2. Rocha TL, Mestre NC, Sabóia-Morais SMT, Bebianno MJ. Environmental behaviour and ecotoxicity of quantum dots at various trophic levels: a review. Environ Int. 2017;98:1-17. http://dx.doi.org/10.1016/j.envint.2016.09.021.
3. Calderón-Garcidueñas L, González-Maciel A, Mukherjee PS, Reynoso-Robles R, Pérez-Guillé B, Gayosso-Chávez C, et al. Combustion- and friction-derived magnetic air pollution nanoparticles in human hearts. Environ Res. 2019;176(June):108567. http://dx.doi.org/10.1016/j.envres.2019.108567.
4. Wang Z, Tang M. The cytotoxicity of core-shell or non-shell structure quantum dots and reflection on environmental friendly: A review. Environ Res. 2021;194:110593. http://dx.doi.org/10.1016/j.envres.2020.110593.
5. Abdallah B, Jazmati AK, Nounou F. Morphological, structural and photoresponse characterization of zno nanostructure films deposited on plasma etched silicon substrates. J. Nanostructures. 2020;10(1):185-97. http://dx.doi.org/10.22052/JNS.2020.01.020.
6. Zhao Y, Ma L, Zhu Y, Qin P, Li H, Mo F, et al. Inhibiting grain pulverization and sulfur dissolution of bismuth sulfide by ionic liquid enhanced poly(3,4-ethylenedioxythiophene): poly(styrenesulfonate) for high-performance zinc-ion batteries. ACS Nano. 2019;13(6):7270-80. http://dx.doi.org/10.1021/acsnano.9b02986.
7. Ajiboye TO, Onwudiwe DC. Bismuth sulfide based compounds: properties, synthesis and applications. Results in Chemistry. 2021;3:100151. http://dx.doi.org/10.1016/j.rechem.2021.100151.
8. Kun WN, Mlowe S, Nyamen LD, Akerman MP, O'brien P, Ndifon PT, et al. Deposition of Bi2S3 thin films from heterocyclic bismuth (III) dithiocarbamato complexes. Polyhedron. 2018;154:173-81. http://dx.doi.org/10.1016/j.poly.2018.07.055.
9. Ahire RR, Sankapal BR, Lokhande CD. Preparation and characterization of Bi2S3 thin films using modified chemical bath deposition method. Mater Res Bull. 2001;36(1–2):199-210. http://dx.doi.org/10.1016/S0025-5408(01)00509-8.
10. Rath AK, Bernechea M, Martinez L, Konstantatos G. Solution-processed heterojunction solar cells based on p-type PbS quantum dots and n-type Bi 2S 3 Nanocrystals. Adv Mater. 2011;23(32):3712-7. http://dx.doi.org/10.1002/adma.201101399.
11. Li Y, Zhang Y, Lei Y, Li P, Jia H, Hou H, et al. In situ fabrication of Bi2S3 nanocrystal film for photovoltaic devices. Mater Sci Eng B. 2012;177(20):1764-8. http://dx.doi.org/10.1016/j.mseb.2012.08.016.
12. Abdallah B, Nasrallah F, Tabbky W. Structural and electrical study of BLT thin film deposited on different substrates by electron gun evaporation. World J. Eng. 2021; ahead-of-print. http://dx.doi.org/10.1108/WJE-06-2020-0200.
13. Díaz-Cruz EB, Cruz-Gómez J, Paraguay-Delgado F, Santos-Cruz J. Improving thermal stability of perovskite solar cell through interface modification by PbS quantum dots. In XVIII Congreso Internacional de Ingeniería Eléctrica, Ciencias de la Computación y Control Automático (CCE). Proceedings. New York: IEEE; 2021. http://dx.doi.org/10.1109/CCE53527.2021.9633033.
14. Ubale AU, Daryapurkar AS, Mankar RB, Raut RR, Sangawar VS, Bhosale CH. Electrical and optical properties of Bi2S3 thin films deposited by successive ionic layer adsorption and

reaction (SILAR) method. Mater Chem Phys. 2008;110(1):180-5. http://dx.doi.org/10.1016/j.matchemphys.2008.01.043.
15. Ubale AU, Shirbhate SC. Electrical, optical and morphological properties of chemically deposited nanostructured HgS-Bi2S3 composite thin films. J Alloys Compd. 2010;497(1–2):228-33. http://dx.doi.org/10.1016/j.jallcom.2010.03.017.
16. Abdallah B, Kakhia M, Obaide A. Morphological and structural studies of ZnO nanotube films using thermal evaporation technique. Plasmonics. 2021;16(5):1549-56. http://dx.doi.org/10.1007/s11468-021-01420-x.
17. Ten Haaf S, Sträter H, Brüggemann R, Bauer GH, Felser C, Jakob G. Physical vapor deposition of Bi2S3 as absorber material in thin film photovoltaics. Thin Solid Films. 2013;535(1):394-7. http://dx.doi.org/10.1016/j.tsf.2012.11.089.
18. Mattox DM. Handbook of Physical Vapor Deposition (PVD) processing. 2nd ed. Burlington: Elsevier; 2010.
19. Denisov VN, Ivlev AN, Lipin AS, Mavrin BN, Orlov VG. Raman spectra and lattice dynamics of single-crystal α-Bi2O3. J Phys Condens Matter. 1997;9(23):4967-78. http://dx.doi.org/10.1088/0953-8984/9/23/020.